Nigerian Research Journal of Chemical Sciences **(ISSN: 2682-6054)**
Volume 8, Issue 2, 2020

SYNTHESIS, ADSORPTION AND INHIBITION BEHAVIOUR OF 2-[(THIOPHEN-2-YLMETHYLIDENE) AMINO] PYRIDINE-3-OL ON MILD STEEL CORROSION IN AGGRESSIVE ACIDIC MEDIA

[1]Nnenna Winifred Odozi, *[2]Festus Chioma and [3]Muhammad Abubakar Dagoli
[1]Department of Chemistry, University of Ibadan, Ibadan, Oyo State, Nigeria
[2]Department of Chemistry, Ignatius Ajuru University of Education, Rumuolumeni, Rivers State, Nigeria
[3]Federal Ministry of Industry, Trade & Investment, Industrial Development Department, Abuja, Nigeria
*Corresponding Author: festchi@yahoo.com

ABSTRACT

The corrosion inhibition and adsorption potentials of 2-[(thiophen-2-ylmethylidene)amino] pyridine-3-ol on mild steel in 1 M hydrochloric acid stood appraised using gravimetric, scanning electron microscopy in addition to quantum chemical techniques. The results acquired in the presence of 100 ppm of the inhibitor at 303 K indicated 97.42% as maximum inhibition efficiency. This implied that inhibition efficiency improved with increase in inhibitor concentration and reduced as the temperature increased. Adsorption of the appraised inhibitor was unprompted as well as consistent with Langmuir adsorption model. Quantum chemical calculations with Density Functional Theory technique was carried out to acquire better insight on the correlation amid inhibitor molecular assemblage plus calculated inhibition efficiency. The quantum chemical parameters calculated were discussed. Scanning electron microscopy evaluation corroborated the establishment of a defensive adsorptive film of the inhibitor on mild steel surface.

Keywords: Adsorption, Corrosion, DFT, Inhibitor, Mild steel

INTRODUCTION

The immense industrial applications of mild steel (ms) based on their special properties have been recognized by many researchers. Ms remains the greatest adopted metallic specie in manufacturing procedures owing to its unequalled weld-ability, machinability, and low cost [1]. Acids typically lead to a corrosive attack in industries during chemical processes [2–5]. The utilization of HCl in preserving of ms, acidification of greasy pits, and also washing off scales remains cost-effective, efficient, and can be likened to other inorganic acids [6]. However, regardless of ms importance, the problem associated with corrosion still remains worrisome. Corrosion remains a foremost challenge confronting countless industries as it offers not just safety hazard [7], but an economic risk to production [8]. It is equally accountable for considerable economic damages in industries hence the demand for techniques to remedy its effect [9]. The main technique for shielding materials in contrast to corrosion, principally in acidic media is the use of inhibitors [10].

Organic compounds consisting of hetero atoms remain the utmost familiar acid inhibitors [11]. The effectiveness of these molecules largely rests on their capacities to be adsorbed on the metallic surface with the polar moieties acting as the reactive centers [12]. The most efficient and proficient inhibitors for metallic species in non-basic medium are heterocyclic compounds bearing chalcogens, pnictogens and cyclic rings [13–15].

Recently, research actions focused on the expansion of less expensive, ecofriendly as well as high efficient corrosion inhibitors. This informed the choice of the inhibitor under study, since it is quite easy to synthesize and contains a reasonable number of active centers.

This research work therefore intends to explore the corrosion inhibitor activity of 2-[(thiophen-2-ylmethylidene)amino] pyridine-3-ol (TMAP) on ms surface in 1 M HCl solution adopting gravimetric technique. The temperature influence of TMAP on corrosion and inhibition procedures were carefully evaluated and deliberated upon. Thermodynamic and kinetic factors were calculated and deliberated. In addition, quantum chemical calculations (QCC) using density functional theory (DFT) and Scanning electron microscopy (SEM) were further assessed in order to advance understanding on the mechanisms of inhibitory procedures.

EXPERIMENTAL

Materials Preparation

The ms adopted for research was cut into different coupons of 4.0 cm x 4.0 cm dimensions. The coupons were washed in dry CH_3CH_2OH and CH_3COCH_3, desiccated at 29 ^oC and kept in a moist free desiccator before usage [16]. The inhibitor-ligand was prepared following a reported procedure [17]. The inhibitor-ligand, 2-[(thiophen-2-ylmethylidene)amino] pyridine-3-ol was synthesized via a one-rung process. Equal quantities of 2-amino-3-hydroxylpyridine (4.96 g, 0.014 mol) dissolved in 20 mL of dehydrated CH_3OH was poured into a stirring solution of thiophene-2-carbaldehyde (0.045mol, 5.0g) agreeing to scheme 1. The resulting reaction mixture stood refluxed for 4 h. On freezing in ice to 27 ^oC, precipitates were gotten, filtered, recrystallized from dehydrated methyl-alcohol and kept *in vacuo* over calcium chloride. The inhibitor-ligand was fully characterized.

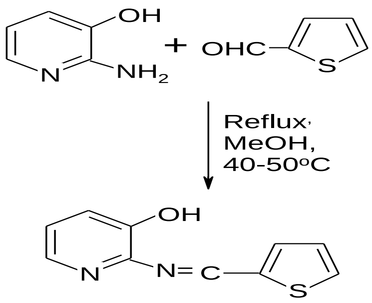

Scheme 1: Synthetic Outline of TMAP Ligand

The concentration range 2 x 10^{-5} to 10 x 10^{-5}M was adopted for the inhibitor. The molecular assemblage of TMAP is presented in Fig. 1.

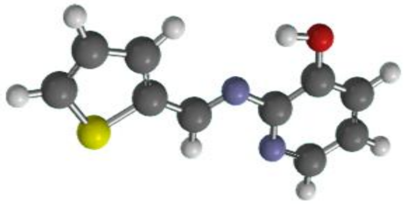

Fig. 1: Perspective view of 2-[(thiophen-2-ylmethyli dene) amino] pyridine-3-ol (TMAP)

Solutions Preparation

Exactly 1 M HCl solution was made via the dilution of 35.4% HCl solvent espousing distilled H_2O. Precisely weighed 0.1 g of TMAP was diluted to 1000 mL in volumetric decanter via distilled H_2O as standard solution (0.1 g/L). The latter was diluted to various concentrations ranging from 2 x 10^{-5} M to 10 x 10^{-5} M as well as the solution devoid of TMAP remained taken as blank for assessment.

Gravimetric Measurement

Gravimetric evaluation was assessed under whole immersion adopting 100 mL sized beakers with 20 mL of the test solution. The pre-determined coupons were submerged into a container comprising the solutions. All coupons remained gradually recovered at 5 h range, washed carefully in 0.2 M sodium hydroxide solution having 200 g/L of Zn-dust with thistle brush, re-washed in distilled H_2O, dehydrated in CH_3COCH_3, and re-determined using an analytical weighing balance. The variation in mass of the coupons afore and afterward submerging in various test solutions remained documented as the weight loss (WL). The test was re-examined at altered temperature. The *WL* data was used in calculating the CR by the relationship [18]:

$$\alpha = \frac{\Delta M}{At} \qquad (1)$$

in which, ΔM represents *WL*, A signifies total area of the ms, t remains corrosion time while **α** ($gcm^{-2}h^{-1}$) is the CR .

Surface Coverage,

$$\Theta = \frac{\alpha 1 - \alpha 2}{\alpha 1} \qquad (2)$$

$$\text{IE} = \frac{\alpha 1 - \alpha 2}{\alpha 1}\ x\ 100\% \qquad (3)$$

where, $\boldsymbol{\alpha_1}$ and $\boldsymbol{\alpha_2}$ are the CR of the ms with and without the inhibitor separately.

Computational Calculations

Spartan' 14 (version 1.2.0) programme at the DFT level by Becke 3 Lee Yang Parr (B3LYP) technique with 6-31G* basis set was espoused in performing quantum-based calculations. The relation amidst IE of inhibitor and the theoretical QC parameters like energy of highest occupied molecular orbital (E_{HOMO}), energy of lowest unoccupied molecular orbital (E_{LUMO}), dipole moment (μ), total energy (TE),, ionization energy (I), electron affinity (A), electronegativity (χ), hardness (η), softness (σ), nucleophilicity (ϖ), fraction of electrons transferred (ΔN) and $E_{LUMO} – E_{HOMO}$ (ΔE) were investigated.

RESULTS AND DISCUSSION

Synthesis

The inhibitor- chelator, [(thiophen-2-ylmethylidene)amino]pyridine-3-ol was obtained in 1:1 mole reaction of 2-amino-3-hydroxylpyridine and thiophene-2-carbaldehyde in methyl-alcoholic solvent. Acquired records (investigative plus spectroscopic) substantiated the structural assemblage of the prepared inhibitor-ligand which was extremely colored and stable at room temperature.

Spectroscopic Data

The inhibitor-ligand displayed intra-chelator bands at 34825 plus 35252; in addition to 25715 plus 23650 cm^{-1} within the UV section apportioned to π* ←□n plus π* ←□ π without *d–d* or LMCT transition observed. The [(thiophen-2-ylmethylidene)amino]pyridine-3-ol inhibitor in its FTIR spectrum presented a broadened band around 3395 cm^{-1} assignable to intra-molecular H-bond (v C–H…N) of azo-methine assemblage giving credibility to [(thiophen-2-ylmethylidene)amino]pyridine-3-ol formation. Similarly, the latter endorses removal of H_2O from the intermediate to give the inhibitor-ligand as well as the non-appearance of amine plus hydroxyl bands frequently spotted in the starting materials. Bands rising from C–H moiety was detected at 3038 cm^{-1}, While the C=N moiety band appeared around 1655 cm^{-1}. The distinguishing band owing to C=C functions resonated as lone band around 1564 cm^{-1}. Bands around 1325, 1115, plus 779 cm^{-1} within the inhibitor-ligand spectrum were characteristic of v(C–N), *v*(C–C) as well as v(C–O) vibrations separately.

CR and IE

The calculated values of CR, θ and IE from gravimetric evaluations at diverse concentrations of the studied inhibitor after 5 h immersion at altered temperature are summarized in Table 1. The temperature influence on CR of TMAP in aggressive 1 M HCl is shown in Fig. 2.

The findings indicate that CR rises with upsurge in temperature but drops with proliferation in concentration of the TMAP. The decline is owing to the inhibitive impacts of the inhibitor that increased through rise in concentration of TMAP. It is obvious (Table 1) that IE improved with increased inhibitor concentration, giving a value of 97.4%. This might be due to the adsorption of TMAP on the ms surface via bonding-free electron pairs of *N*- and *O*-atoms plus pi-electrons of the cyclic rings in addition to the imine moiety. Extreme inhibitive proficiency of TMAP corroborates a strong bonding capability of the inhibitor to the ms surface.

Table 1: Effect of Temperature on corrosion rate on ms in 1M HCl solution of varied concentrations of TMAP

TMAP	**303 K**			**313 K**			**323 K**			**333 K**			**343 K**		
C (ppm)	**IE (%)**	**C_R (10^{-4})**	**θ**	**IE (%)**	**C_R (10^{-4})**	**Θ**	**IE (%)**	**C_R (10^{-4})**	**θ**	**IE (%)**	**C_R (10^{-4})**	**Θ**	**IE (%)**	**C_R (10^{-4})**	**θ**
0	-	74.5	-	-	114.2	-	-	242.0	-	-	248.8	-	-	265.4	-
20	80.2	14.8	0.80	54.1	52.4	0.54	40.0	145.0	0.40	29.4	175.6	0.29	24.9	199.4	0.24
40	83.1	12.6	0.83	73.9	27.9	0.73	54.6	109.6	0.54	39.6	150.3	0.39	42.8	158.9	0.42
60	87.6	9.2	0.87	79.6	23.3	0.79	60.0	96.5	0.60	43.4	140.8	0.43	43.8	149.0	0.43
80	95.9	3.0	0.95	84.8	17.4	0.84	63.4	88.5	0.63	56.8	107.4	0.56	48.7	136.2	0.48
100	**97.4**	1.9	0.97	86.8	15.1	0.86	65.2	84.1	0.65	63.2	91.7	0.63	53.6	123.3	0.53

C_R - CR (g/cm^2/h); IE - IE (%); θ - Degree of Θ

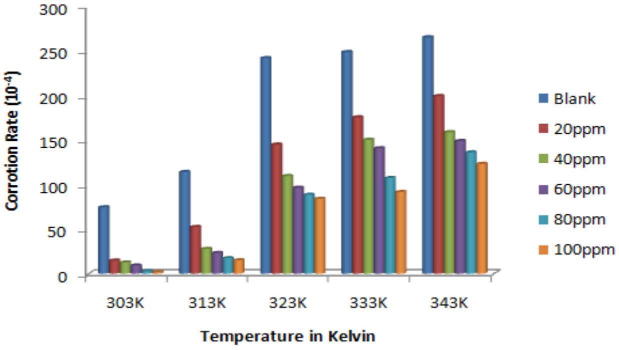

Fig. 2: Temperature influence on CR of TMAP in 1 M HCl

Variation of IE against Concentrations of TMAP at 303 – 333K

The plot of IE against concentration is displayed in Fig. 3. The data revealed that increase in IE corroborates rise in concentration denoting that TMAP act through the establishment of a barrier layer amidst the metallic specie and the corrosive intermediate by its adsorption on the ms surface. Thus, the nature of adsorption (physical or chemical adsorption) has been confirmed by the thermodynamic parameters as discussed in subsequent sections.

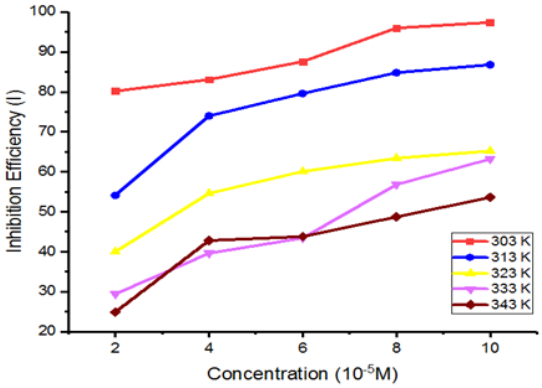

Fig. 3: Variation of IE against concentrations of TMAP at 303 – 333K

Adsorption Studies

Corrosion inhibition (C_I) is a surface phenomenon. The interface of surface inhibitor can be evaluated via its investigational data. The IE depends on the nature, amount of energetic sites within the metallic surface, charge density, molecular size of inhibitor, metallic-inhibitor interfaces plus the metallic complex assemblage. Adsorption isotherms afford data on the metallic inhibitor interfaces [19]. The utmost recurrently espoused remain those of Langmuir, Temkin, Freundlich, El-Awady, Frumkin, Parsons, Flory–Huggins as well as Bockris–Swinkels. The models considered were [16]:

Langmuir isotherm: $\theta = K_{ads} C$ (4)

Temkin isotherm: $\exp(f\theta) = K_{ads} C$ (5)

The adeptness of TMAP as corrosion inhibitor could be ascribed to the existence of electron donor atoms like nitrogen, oxygen or sulphur within the molecular assemblage, which favour its adsorption on the metallic surface. Some of the adsorption isotherms were fitted but best fit was acquired for Langmuir adsorption isotherms.

Langmuir adsorption isotherm (LAI) on ms CI by TMAP inhibitor

The studies indicate that the adsorption follows LAI. A plot of C/θ against C (Fig. 4) afforded a straight line ($R^2 > 0.9$) graph suggesting that the linear correlation coefficients (R^2) were practically equivalent to 1 thereby corroborating the fact that the adsorption of TMAP on ms surface was consistent with LAI. It also revealed that the organic compounds on the inhibitor molecule with polar atoms or groups adsorbed on the metallic surface and interact by shared repulsion or attraction [19].

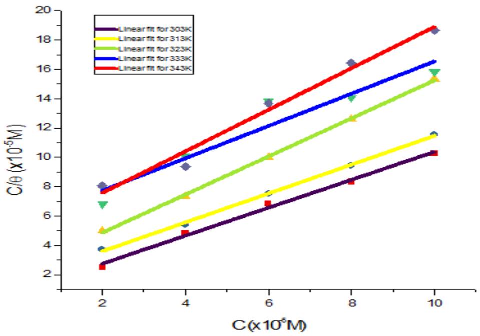

Fig. 4. Langmuir adsorption isotherm of TMAP on ms in 1M HCl at 303 – 343K

Temkin adsorption isotherm on ms CI by TMAP inhibitor

According to Temkin isotherm, the plot of ϴ acquired from *WL* technique against ln C (M) at dissimilar concentrations of the inhibitor showed a straight line, which is graphically represented in Fig. 5. It is observed that the adsorption of TMAP on ms surface follows the Temkin adsorption isotherm. From Temkin adsorption parameters, 'a' and 'K_{ads}' are molecular interaction parameter and equilibrium constant of adsorption process respectively. The calculated values figured out from Temkin adsorption plot (Fig. 5) is displayed in Table 3. Also, the parameter 'f' is defined as:

$$f = -2a \tag{6}$$

in which f denotes non-homogeneous factor of ms surface indicating the molecular interactions in the adsorption layer. It is evidently defined from Equation 6 that, if $a < 0$, then $f > 0$; if $a > 0$, then $f < 0$. Thus, if $f < 0$ attraction of molecules take place and if $f > 0$, mutual repulsion of molecules occurs [16].

The adsorption studies revealed that the adsorption equilibrium constant (K_{ads}) drops with rise in T, which shows that, TMAP adsorbed easily on the ms surface at lower T. At higher T, the adsorbed inhibitors are likely to desorb from the ms surface [20]. The low values of K_{ads} shown in Tables 2 and 3 indicate weak interaction between TMAP plus the ms surface. This submits that electrostatic interface (Physisorption) amidst the inhibitor molecules plus the ms surface prevailed over molecular interface leading to strong interactions (Chemisorption) [16]. Equation 7 shows the correlation amid the equilibrium constant of adsorption (K_{ads}) and that of the standard free energy of adsorption (ΔG_{ads}).

$$K_{ads} = \frac{1}{55.5} \exp\left(\frac{-\Delta Gads}{RT}\right) \tag{7}$$

Equation 7 is rearranged to equation 8

$$\Delta G_{ads} = -RT \ln(55.5 \times K_{ads}) \tag{8}$$

Equation 8 was used in calculating the ΔG_{ads} as displayed in Tables 2&3. The non-positive dta arising from ΔG_{ads} reveal impulsiveness of the adsorption manner as well as firmness of the adsorbed layer on the ms surface. Values of ΔG_{ads} up to – 20 kJ/mol remain related to electrostatic interaction amidst the charged molecules and the metallic specie (Physisorption), while those non-positive values of ΔG_{ads} greater than – 40 kJ/mol suggest sharing or transfer of electrons from the inhibitors to the metallic surface to establish a coordinate bond type (Chemisorption) [21].

From Table 2 and 3, the experimental values of ΔG°_{ads} was observed to be less than –20 kJ/mol, indicating that the adsorption of TMAP on ms surface in 1M HCl solution was typically physisorption.

Table 2: Langmuir adsorption parameters for ms in 1M HCl at different concentrations of TMAP at 303 – 343 K

Inhibitor	**T (K)**	**Langmuir Adsorption Parameters**				
		Slope	**Intercept**	**K_{ads}**	**ΔG_{ads}(kJ/mol)**	**R^2**
TMAP	303	0.95	0.83	1.20	-10.59	0.995
	313	0.98	1.61	0.62	-9.21	0.999
	323	1.30	2.26	0.44	-8.60	0.999
	333	1.10	4.32	0.23	-7.07	0.919
	343	1.42	4.74	0.21	-7.02	0.979

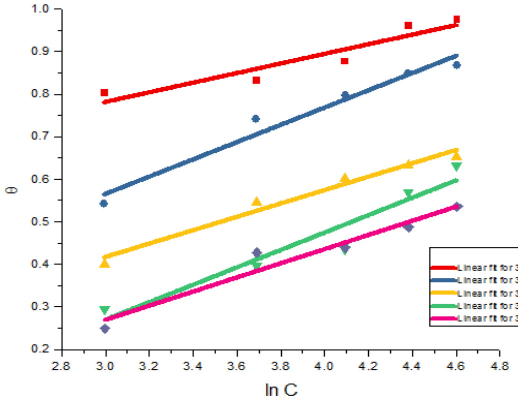

Fig. 5. Temkin adsorption isotherm of TMAP on ms in 1M HCl at 303 – 343K

Table 3: Temkin adsorption parameters for ms in 1M HCl at different concentrations of TMAP at 303 – 343K

Inhibitor	**T (K)**	**TemkinAdsorption Parameters**						
		Slope	**Intercept**	***f***	***a***	**K_{ads}**	**ΔG_{ads}(kJ/mol)**	**R^2**
TMAP	303	0.11	0.44	8.85	-4.43	50.14	-19.98	0.885
	313	0.20	-0.04	4.93	-2.47	0.81	-9.90	0.966
	323	0.16	-0.05	6.36	-3.18	0.71	-9.85	0.972
	333	0.20	-0.34	7.89	-2.44	1.15	-11.51	0.922
	343	0.17	-0.23	6.01	-301	0.25	-7.51	0.944

Kinetic/Thermodynamic Considerations

The calculated CR data at 303 – 343K examined fits into Arrhenius equation signifying that the rate of a reaction is temperature dependent. The activation parameters for the corrosion process were evaluated on the basis of Arrhenius type equation:

$$C_R = A \exp^{-Ea/RT} \tag{9}$$

Taking the logarithm of both sides of equation 9, equation 10 is obtained

$$\text{Log } C_R = \text{Log } A - E_a/2.303RT \tag{10}$$

Where E_a denotes activation energy, *A* signifies Arrhenius or pre-exponential factor, T represents temperature and R stands for molar gas constant. Fig. 6 is a plot of Log C_R against $1/T$ which affords straight lines, with slope of $-Ea/2.303R$ and intercept of Log *A*. Also, Table 4 displayed the activation parameters calculated from the plot.

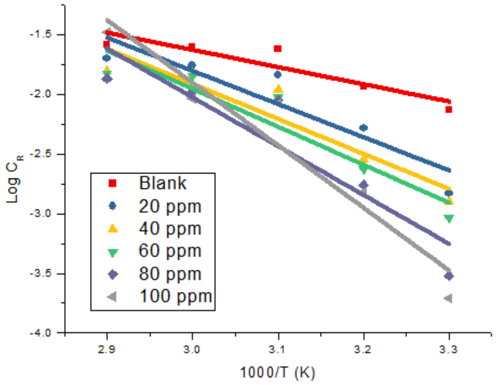

Fig. 6: A plot of Arrhenius of Log C_R against 1/T for ms in 1M HCl comprising diverse concentration of TMAP

Equation 11 is a transition state equation giving the thermodynamics parameters (Table 4) of enthalpy, ΔH^*_{ads} and entropy, ΔS^*_{ads} which were calculated from a plot of Log C_R/T against 1/T as presented in Fig. 7.

$$C_R = \frac{RT}{Nh} \exp \frac{\Delta S*}{R} \exp \frac{-\Delta H*}{RT} \tag{11}$$

The enthalpy and entropy of the system was calculated from the slope ($-\Delta H^*_{ads}/R$) and the intercept $\{\ln(R/Nh) + (\Delta S^*_{ads}/R)\}$ of the plot respectively.

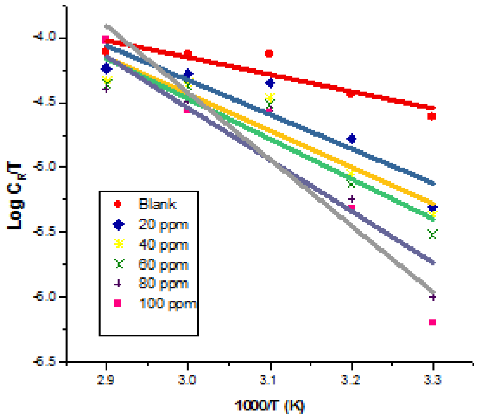

Fig. 7: A plot of Transition state of Log C_R/T versus 1/T for ms in 1M HCl containing dissimilar concentration of TMAP

Table 4 clearly indicates that E*a* is lowermost for the solution in the absence of acid but higher with the TMAP. The E*a* values increased as the inhibitor concentration (20–100 ppm) improved. This might be accredited to an improved energy barrier for the ms corrosion implying that the ms dissolution decreased in the presence of TMAP due to the adsorption of inhibitors on the high energy surface sites, barring the active sites. The non-negative values of ΔH^*_{ads} obtained indicates the endothermic kind of corrosion process which is consistent with slow dissolution of the ms [16]. Generally, enthalpy with lower values indicates physical adsorption while that with higher values above 100kJ/mol indicates chemical adsorption [22]. This study also revealed that the absolute enthalpy values acquired were corroborative of physisorption process for all concentrations of TMAP. The negative values of the entropy of adsorption, ΔS^*_{ads} (Table 4) acquired indicates that the adsorption process decreases in disorder for the systems owing to adsorption of fragments of TMAP on the ms surface. The decline in entropy of adsorption arose from the free movement of TMAP molecules in the bulk solution that were adsorbed in an organized manner onto the metallic surface. The study also revealed that the activated complex in the rate determining step depicts a connection somewhat than a dissolution step, indicating that a decline in disorder occurs on moving from reactants to the activated complex [23].

Table 4: Thermodynamic parameters for ms corrosion in 1 M HCl with and without TMAP inhibitor

TMAP Concentration (ppm)	**E_a (kJ/mol)**	**ΔH^o (kJ/mol)**	**ΔS^o (J/mol/K)**
Blank	27.57	25.08	- 181.06
20	53.23	50.55	- 168.47
40	56.10	53.61	- 157.97
60	60.89	58.61	- 145.91
80	78.31	75.82	- 115.54
100	100.33	98.03	- 40.31

Scanning Electron Microscope

SEM technique remains adopted in investigating the morphology of the ms surface after immersion in 1 M HCl with and without 100 ppm of TMAP at 303 K for 3 h as shown in Fig. 8. It was found that a rough surface was observed in corrosive solution without TMAP owing to high decompose average of ms surface (Fig.8a), whereas thin film covered the ms surface by addition of 100 ppm concentration of TMAP giving a smoother surface (Fig.8b). These indications disclose that the inhibitor establishes defensive layer on the ms surface, which inhibits the attack of acid and the dissolution of ms by forming surface adsorbed layer and thereby reducing the CR.

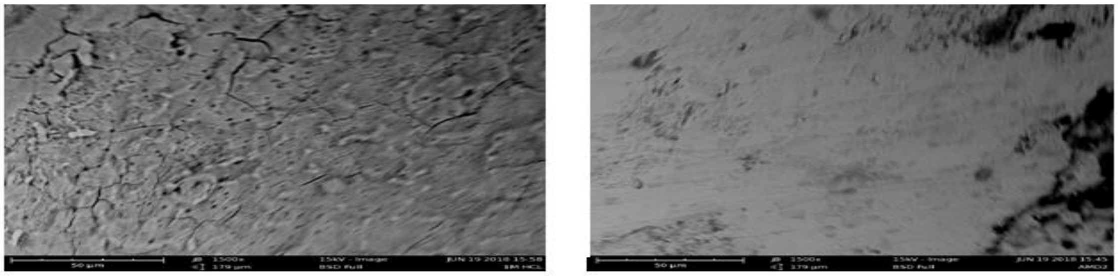

(a) (b)

Fig. 8: SEM micrographs of ms surface in 1M HCl in the absence and presence of 100 ppm of TMAP at 303 K

Quantum Chemical Approach

QCP and Mullikan charge distribution are shown in Tables 5 and 6 respectively. Fig. 9 – 11 displays the HOMO and LUMO energies and electrostatic potential map (ESPM) respectively for TMAP molecule. Generally, relationship between IE of corrosion inhibitors and molecular parameters like E_{HOMO}, E_{LUMO} and ΔE are explored to obtain data on the reactive nature of a molecule as the reactive potentials of an inhibitor is strictly linked to its frontier molecular orbitals, HOMO and LUMO [24]. The region of electron density that is usually related to electron giving capability of a molecule is referred to as HOMO while the region related to electron accepting potential is referred to as LUMO [24].

Recent literature highlighted that greater E_{HOMO} of the inhibitor implies enhanced capability to donate electrons to empty *d*-orbitals of the metallic ion and the greater the corrosion IE. Table 5 demonstrates that TMAP has a high E_{HOMO}, which indicates that the interaction between the inhibitor and the ms is electrostatic (i.e. physisorption) in nature, thus corroborating the experimental results obtained. It also designates that the adsorption of TMAP onto the ms surface is aided, so, confirming a smooth transport process through the adsorbed layer. The energy gap (ΔE) is the difference between the E_{LUMO} and E_{HOMO} and is a vital stability index [11].

Table 5: Calculated *QCP* of the inhibitor TMAP

Quantum Chemical Parameters	**TMAP**
TE (au)	- 968.7753
E_{HOMO} (eV)	- 5.70
E_{LUMO} (eV)	- 2.08
ΔE_{gap} (eV)	3.62
μ (Debye)	1.58
I (eV)	5.70
A (eV)	2.08
χ (eV)	3.89
Fraction of Electron Transferred ΔN	0.8591

Furthermore, ΔE is also connected to hardness or softness of a molecule. While soft molecules are more reactive compared to hard molecules, the energy required to eliminate an electron from the last occupied orbital is very low [4]. Low value of ΔE corroborates enhanced IE. The result in Table 5 specifies lower value of ΔE, which implies good IE, and less required energy for electron removal [25]. The study also reveals that TMAP exhibits improved chemical reactivity, lower kinetic steadiness, more polarized and thus referred to as a soft molecule. High ionization energy (I = 5.70 eV) designates enhanced steadiness [26], number of electrons donated (ΔN) were also evaluated and tabulated in Table 5. $\Delta N < 3.6$ suggests that the inhibitor may also possess the tendency to transfer electrons to the ms surface [27].

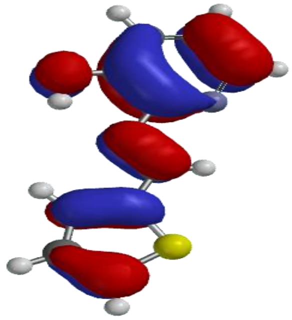

Fig. 9: HOMO of TMAP molecule

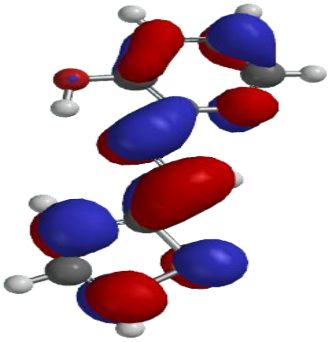

Fig. 10: LUMO of TMAP molecule

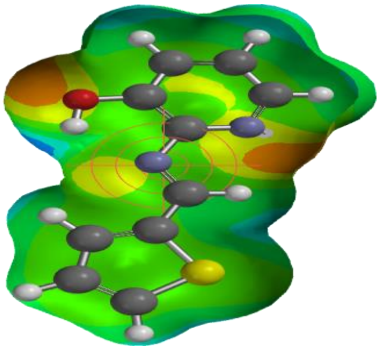

Fig. 11**:** ESPM of TMAP molecule

Table 6 shows the Mullikan charge distribution of TMAP molecule. It is revealed from literature that the high non-positive the atomic charges of the adsorbed centre are, the greater the atom gives its electron to the empty *d*-orbitals of the metallic [28] ion. The data obtained in Fig.9 and 10 show that *N*-, *O*- and some carbon atoms possess great non-positive charges corroborating that they are the active centres, with strong ability to bond onto the ms surface. The ESPM of TMAP molecule is shown in Fig. 11, which is in good agreement with the Mullikan charge distribution due to the fact that *O*- and *N*- atoms fall under the electron rich region in the electrostatic potential map. Generally, the electron rich section is red followed by orange, green and the electron less section is blue for the TMAP molecule.

Table 6**:** The atoms in TMAP molecule and their Mullikan charges

Atom	Charges
C1	0.076163
C2	-0.154032
C3	-0.100211
C4	-0.098251
C5	0.460481
C6	-0.338928
C7	-0.151935

C8	0.305539
C9	-0.132449
C10	0.030685
N1	-0.533382
N2	-0.647621
O1	-0.647621
S1	0.274042
H1	0.171361
H2	0.156326
H3	0.151125
H4	0.181953
H5	0.138693
H6	0.151027
H7	0.137850
H8	0.421655

CONCLUSIONS

- The data obtained from the investigational and hypothetical evaluations showed that TMAP was effective and efficient as an inhibitor for ms corrosion in hydrochloric acidic medium with an IE of 97.4%.
- The IE of TMAP increased with rise in concentration of TMAP and however reduced with rise in T.
- CR increases as temperature rises both with and without the inhibitor but reduces more with the inhibitor.
- The adsorption of TMAP on ms surface of 1M HCl obeys the Langmuir adsorption model at all the concentrations and temperatures studied.
- The phenomenon of physical adsorption is proposed from the values of kinetic/thermodynamics parameters obtained.
- SEM micrographs showed that the inhibitor molecule form a good protective film on surface of the ms.
- Data obtained from QCC using DFT was reasonably in good agreement with the investigational data.

Acknowledgements

The authors acknowledged Dr N.W. Odozi for carrying out the computational section and Dr. Chioma Festus for the freshly prepared inhibitor adopted for the research work.

REFERENCES

[1] Singh, P. Quraish, M.A. Gupta, S.L. & Dandia, A. (2016). Investigation of the *CI* effect of 3-methyl-6-oxo-4-(thiophen-2-yl)-4,5,6,7-tetrahydro-2H-pyrazolo[3,4b]pyridine-5-carbonitrile (TPP) on mild steel in hydrochloric acid, *Journal of Taibah University of Sciences*, 10(2016), 139–147.

[2] Solmaz, R. (2014). Investigation of adsorption and corrosion inhibition of mild steel in Hydrochloric acid solution by 5-(4-dimethylaminobenzylidene) rhodanine, *Corrosion Sci.*. 79, 169–176.

[3] Ren, Y. Luo, Y. Zhang, K. Zhu, G. & Tan, X. (2008). Lignin terpolymer for corrosion inhibition of mild steel in 10% hydrochloric acid medium, *Corrosion Sci.*, 50, 3147–3153.

[4] Umoren, S.A. Ogbobe, O. Igwe, I. O. & Ebenso, E.E. (2008). Inhibition of mild steel corrosion in acidic medium using synthetic and naturally occurring polymers and synergistic halide additives, *Corrosion Sci.*, 50, 1998–2006.

[5] Adejoro, I.A. Ojo, F.K. & Obafemi, S.K. (2015). Corrosion inhibition potentials of Ampicillin for mild steel in hydrochloric acid solution, *Journal of Taibah University of Sciences*, 9(2), 192–202.

[6] Singh, D.D. Singh, T.B. & Gaur, B. (1995). The role of metal cations in improving the inhibitive performance of hexamine on the corrosion of steel in hydrochloric acid solution, *Corros. Sci.* 37, 1005–1019.

[7] Abbasov, V.M. Abd El-Lateef, H.M. Aliyeva, L.I. Ismayilov, I.T. Qasimov, E.E. & Narmin, M.M. (2013). Efficient Complex Surfactants from the Type of Fatty Acids as Corrosion Inhibitors for Mild Steel C1018 in CO_2-Environments, *J. Korean Chem. Soc.* 57, 25–34.

[8] Desimone, M. Grundmeier, G. Gordillo, G. & Simison, S. (2011). Amphiphilicamido-amine as an Effective Corrosion Inhibitor for Mild Steel Exposed to CO_2 Saturated Solution: Polarization, EIS and PM-IRRAS studies, *Electro. Act.*, 56, 2990–2998.

[9] Elron, E.G. (2015). *Green Inhibition of mild steel in CO_2 saturated saline solution*, Ph.D Thesis, Amer. Uni. Sharjah, UAE.

[10] Trabanelli, G. (1991). Whitney Award Lecture: Inhibitors – An Old Remedy for a New Challenge, ***Corros. Sci.,*** 47, 410–419.

[11] Odozi, N.W. Babalola, J.O. Ituen, E.B. & Eseola, A.O. (2015). Imidazole Derivative as Novel

Effective Inhibitor of Mild Steel Corrosion in Aqueous H_2SO_4 Acid. *American J. Phys. Chem.***,** 4, 1–9.

[12] Elkadi, L. Mernari, B. Traisnel, M. Bentiss, F. & Lagrenee, M. (2000). The inhibition action of 3,6-bis(2-methoxyphenyl)-1,2-dihydro-1,2,4,5-tetrazine on the corrosion of mild steel in acidic media, *Corros. Sci.,* 42, 703–719.

[13] Shukla, S.K. Quraishi, M.A. & Prakash, R. (2008). A self-doped conducting polymer polyanthranilic acid: an efficient corrosion inhibitor for mild steel in acidic solution, *Corros. Sci*., 50, 2867–2872.

[14] Abdallah, M. & El-Naggar, M.M. (2001). Cu^{+2} cation+3, 5-dimethyl pyrazole mixture as a corrosion inhibitor for carbon steel in sulfuric acid solution, *J. Mat. Chem. Phys.*, 71, 291–298.

[15] Fouda, A.S. & Ellithy, A. S. (2009). Inhibition effect of 4-phenylthiazole derivatives on corrosion of 304L stainless steel in HCl solution, *Corros. Sci.* 51, 868–875.

[16] Obi-Egbedi, N.O. Obot, I.B. El-Khaiary, S.A. & Ebenso, E.E. (2011). Computational Simulation and Statistical Analysis on the Relationship between Corrosion Inhibition Efficiency and Molecular Structure of Some Phenanthroline Derivatives on Mild Steel Surface, *Int. J. Electro. Sci.***,** 6, 5649–5675.

[17] Festus, C. (2017). Synthesis, Characterization and Antibacterial Studies of Heteroleptic Co(II), Ni(II), Cu(II) and Zn(II) Complexes of N-(2-hydroxybenzylidene)pyrazine-2-carboxamide. *International Journal of Chemistry, Pharmacy & Technology*, 2(5), 202-211.

[18] Obot, I.B. & Obi- Egbedi, N.O. (2010). Adsorption properties and inhibition of mild steel corrosion in sulphuric acid solution by ketoconazole: Experimental and theoretical investigation, *Corros. Sci.*, 52,198–204.

[19] Manimegalai, S. & Manjula, P. (2015). Thermodynamic and adoption studies for corrosion inhibition of mild steel in aqueous media by Sargasam Swartzii (Brown Algae), *J. Mat. Environ. Sci.***,** 6, 1629–1637

[20] Hegazy, M.A. Ahmad, H.M. & El- Tabei, A.S. (2011). Investigation of the inhibitive effect of p-substituted 4-(N,N,N-dimethyldodecylammonium bromide)benzylidene-benzene-2-yl-amine on corrosion of carbon steel pipelines in acidic medium, *Corros. Sci***.** 53, 671 – 678.

[21] Li, X. Deng, S. & Fu, H. (2011). Inhibition by tetradecylpyridinium bromide of the corrosion of aluminium in hydrochloric acid solution, *Corros. Sci.* 53, 1529–1536.

[22] Martinez, S. & Stern, I.J. (2001). Thermodynamics studies of Azardirachtaindicatae, *Appl. Electrochem***.** 31, 973–978.

[23] Herrag, L. Hammouti, B. Elkadiri, S. Aouniti, A. Jama, C. Vezin, H. & Bentiss, F. (2010). Adsorption properties and inhibition of mild steel corrosion in hydrochloric solution by some newly synthesized diamine derivatives: Experimental and theoretical investigations, *Corros. Sci.*, 52, 3042–3051.

[24] Obot, I.B. Obi-Egbedi, N.O. Umoren, S.A. & Ebenso, E.E. (2010). Synergistic and Antagonistic Effects of Anions and Ipomoea invulcrata as Green Corrosion Inhibitor for Aluminium Dissolution in Acidic Medium, *Int. J. Electro. Sci.*, 5, 994–1007.

[25] Gece, G. (2008). The use of quantum `chemical methods in corrosion inhibitor studies, *Corros. Sci.* 50, 2981 – 2992.

[26] Dwivedi, A. & Misra, N. (2010). Quantum chemical study of Etodolac (Lodine), *Der Pharma Chemica*, 2, 58 – 65.

[27] Hjouji, M.Y. Djedid, M. Elmsellem, H. KandriRodi, Y. Ouzidan, Y. Ouazzani, C. Sebbar, N.K. Essassi, E.M. Abdel-Rahman, I. & Hammouti, B. (2016). Corrosion Inhibition of mild steel in hydrochloric acid solution by pyrido[2,3-b]pyridine derivative: electrochemical and theoretical evaluation**.** *J. Mater. Environ. Sci***.** 7, 2028-2508.

[28] Xia, S. Qiu, M. Yu, L. Liu, F. & Zhao, H. (2008). Molecular dynamics and density functional theory study on relationship between structure of imidazoline derivatives and inhibition performance. *Corros. Sci.*, 50, 2021–2029.